Suppressing void defects in long wavelength semipolar $(20\bar{2}\bar{1})$ InGaN quantum wells by growth rate optimization

Yuji Zhao,[1,a)] Feng Wu,[2] Chia-Yen Huang,[2] Yoshinobu Kawaguchi,[2] Shinichi Tanaka,[2] Kenji Fujito,[3] James S. Speck,[2] Steven P. DenBaars,[1,2] and Shuji Nakamura[1,2]
[1]*Electrical and Computer Engineering Department, University of California, Santa Barbara, California 93106, USA*
[2]*Materials Department, University of California, Santa Barbara, California 93106, USA*
[3]*Optoelectronic Laboratory, Mitsubishi Chemical Corporation, 1000 Higashi-Mamiana, Ushiku, Ibaraki 300-1295, Japan*

(Received 15 January 2013; accepted 22 February 2013; published online 6 March 2013)

We report on void defect formation in $(20\bar{2}\bar{1})$ semipolar InGaN quantum wells (QWs) emitting in the green spectral region. Fluorescence and transmission electron microscopy studies indicate that this type of defect is associated with voids with $\{10\bar{1}1\}$, $\{10\bar{1}0\}$, and $\{000\bar{1}\}$ side facets in the QW region. Systematic growth studies show that this defect can be effectively suppressed by reducing the growth rate for the active region. Green light-emitting diodes (LEDs) with reduced active region growth rate showed enhanced power and wavelength performance. The improved LED performance is attributed to the absence of void defects in the active region. © *2013 American Institute of Physics*. [http://dx.doi.org/10.1063/1.4794864]

Nonpolar (NP) and semipolar (SP) growth of the (Al,Ga,In)N-based semiconductors are attractive for the fabrication of long wavelength light-emitting diodes (LEDs) and laser diodes (LDs), due to the reduction of the quantum confined Stark effect (QCSE) in the quantum wells (QWs).[1–4] NP and SP devices have higher radiative recombination rate and reduced wavelength shift with increasing carrier injection in comparison with conventional *c*-plane (0001) LEDs.[5–7] Growth of high-indium-content NP and SP QWs, however, often leads to the formation of the extended defects, e.g., misfit dislocations (MDs) and basal plane stacking faults (BPSFs), at highly mismatched interfaces.[8] These defects, which commonly act as nonradiative recombination centers, are extremely detrimental to optoelectronic device performance. Understanding the defect generation mechanisms and their suppression methods are therefore essential for developing high performance NP and SP LEDs and LDs in the long wavelength region.

Recently, several SP orientations have shown improved defects tolerance and material quality for the growth of long wavelength InGaN QWs.[9] The SP $(20\bar{2}1)$ plane has been used to produce high performance green LEDs and LDs.[3,4,9] It was argued that InGaN layer grown on this plane exhibit a high degree of homogeneity even with high indium content.[3] Several other advantageous features, including high optical polarization, high indium incorporation, and small wavelength shift, were recently reported on $(20\bar{2}\bar{1})$ green LEDs and LDs.[10–13] However, due to the increased lattice mismatch, defect generation was almost inevitable for high-indium-content SP InGaN QWs, which resulted in a reduced overall device performance in the green and yellow spectral region. Structural defects such as dislocations, V-defects, and stacking faults have already been found on *c*-plane and *m*-plane GaN-based heterostructures.[8,14] However, there are few reports on structural defects on SP InGaN QWs. Recently, $(20\bar{2}\bar{1})$ SQW LEDs have attracted attention due to the low droop performance in the blue region. However, black triangular defects were observed for $(20\bar{2}1)$ SQW LEDs when the device wavelength extends to the green spectral region. Similar defects were also observed for $(20\bar{2}1)$, $(30\bar{3}1)$, and $(30\bar{3}\bar{1})$ SP devices. In this paper, we investigate the defect formation in the long wavelength (>500 nm) SP $(20\bar{2}\bar{1})$ InGaN/GaN QWs. Black triangular defects with feature dimension of 10 to 50 μm were observed for green SQW $(20\bar{2}\bar{1})$ LEDs under fluorescence (FL) microscopy (this defect has been observed frequently in our laboratory for many SP orientations). Transmission electron microscopy (TEM) studies demonstrate that these black triangular defects were composed of a high density ($\sim 10^9/\text{cm}^2$) of 50 to 100 nm voids in the active region. Systematic growth studies show that these defects can be effectively eliminated by growth rate optimization.

LED structures were grown by conventional metal organic chemical vapor deposition (MOCVD) on free-standing $(20\bar{2}\bar{1})$ GaN substrates supplied by Mitsubishi Chemical Corporation. The device structure consisted of a 1 μm Si-doped *n*-type GaN layer, 15 sets of $In_{0.01}Ga_{0.99}N$ (2.5 nm)/GaN (2.5 nm) superlattice, an InGaN single quantum well (SQW) active region, an 8 nm Mg-doped $Al_{0.15}Ga_{0.85}N$ electron blocking layer (EBL), and a 40 nm *p*-type GaN layer. The emission wavelengths of the InGaN SQW are in the range of 500 to 510 nm. First, to study defect formation conditions, SQW LED structures with different QW thickness (2 nm, 4 nm, 6 nm) were grown on under the same conditions. The corresponding electroluminescence (EL) intensity of the LEDs decreased with increasing QW thickness. The FL and optical microscopy images for the devices are summarized in Figs. 1(a)–1(f), where a high density of black triangular defects were observed on 4 nm and 6 nm QW samples. The FL microscopy has similar structure with the optical microscopy except that a light source (a mercury lamp) and filter blocks are used for observation. The wavelengths for excitation filter

a)Electronic mail: yujizhao@engineering.ucsb.edu.

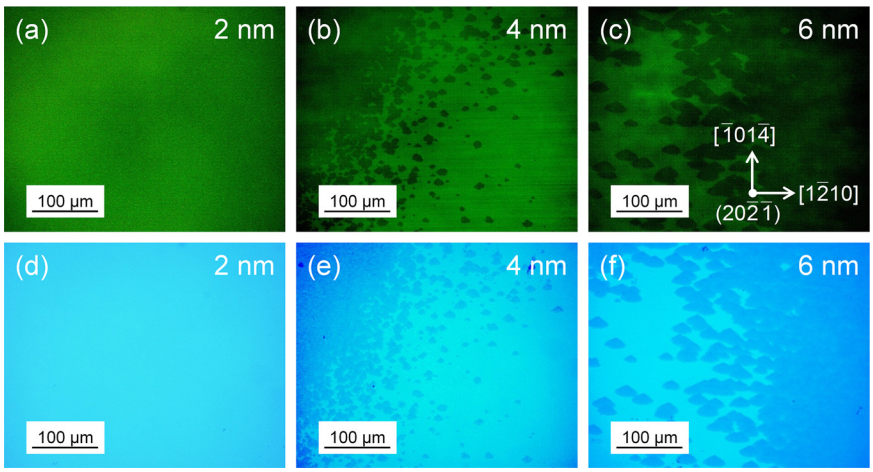

FIG. 1. FL and optical microscopy for semipolar (20$\bar{2}$1) SQW LEDs with a QW thickness of (a),(d) 2 nm, (b),(e) 4 nm, and (c),(f) 6 nm.

(EX), dichroic mirror (DM), and barrier filter (BA) of the FL microscopy are 380 to 420 nm, 430 nm, and 450 nm, respectively. To investigate the origin of reduction in EL power, the 6 nm QW LED was selected for TEM characterization. Second, to explore the suppression technique for such defects, 3 nm SQW (20$\bar{2}$1) LEDs with different growth rate (GR = 1 Å/s, 0.3 Å/s, 0.15 Å/s) were grown by MOCVD. Quick test EL measurements were performed on these samples by depositing ~1 mm diameter indium dots on the top of the *p*-GaN as contacts. Third, to study the effect of growth rate on material properties, (20$\bar{2}$1) samples with 3 sets of InGaN (3 nm)/GaN (10 nm) QWs were grown under fast (GR = 1 Å/s) and slow growth rate (GR = 0.15 Å/s). Atomic force microscopy (AFM) and secondary ion mass spectrometry (SIMS) characterization were performed on the samples.

Figures 1(a)–1(f) demonstrate FL and optical microscopy images for (20$\bar{2}$1) SQW LEDs with QW thickness of 2 nm, 4 nm, and 6 nm, respectively. All of the samples showed green luminescence under FL, which is consistent with emission wavelengths of the devices (500–510 nm). At a QW thickness of 2 nm, the LEDs exhibited uniform luminescence, while black triangular defects were observed for the 4 nm and 6 nm SQW LEDs. To further study the microstructure of the defects, the 6 nm QW LED sample was selected for TEM characterization. Figures 2(a) and 2(b) demonstrate two beam scattering contrast images in [1$\bar{2}$10] cross-sectional TEM with $\mathbf{g} = 10\bar{1}0$ diffraction condition. The TEM images show that these defects are dish-like microstructural voids (cross-sectional dimension of 50 to 100 nm) with clear {10$\bar{1}$1}, {10$\bar{1}$0}, and {000$\bar{1}$} internal facets. These facets are consistent with the previous reports of the facet planes on V-defects and pyramid void defects from *c*-plane devices.[14,15] Figure 2(c) shows a [$\bar{1}$014] cross-sectional TEM of the sample. However, no clear facets were observed in this cross-section. The defects initiate below the bottom of the QW and remain empty throughout the whole QW region. A high density of voids (~10^9/cm^2) were found under the dark triangular surface area. Figure 2(d) shows the schematic view of one example of the defect on SP (20$\bar{2}$1) plane in a wurtzite crystal structure. The formation of these void defects, possibly originated during the InGaN growth, was further exacerbated by the high temperature growth of EBL and *p*-GaN layer after the active region.[16] BPSFs and MDs were also observed on the samples; however, it is still unclear whether they are related to void defects. It is a topic of ongoing investigation.

Different growth techniques have been explored to suppress this type of void defect for long wavelength SP QWs. In our previous studies, such defects in the InGaN QWs can be effectively reduced or eliminated using an AlGaN quantum barrier.[4] However, the significant difference between the optimal growth temperatures between high-indium-content QWs and AlGaN barriers limited the achievable improvement. Low barrier growth temperature results in poor crystal quality of AlGaN barrier while an excessively high growth temperature causes thermal damage to the QWs. For high performance green light emitters, high quality InGaN QWs with simple Al-free GaN barrier is desirable. To explore the best growth condition for such a structure, SQW SP (20$\bar{2}$1) InGaN/GaN LEDs were grown with a different growth rate by MOCVD. The triethygallium (TEG) flow for the active region of the devices was varied from 30 to 5 SCCM, the corresponding growth rate was 1 Å/s, 0.3 Å/s, and 0.15 Å/s, respectively, as confirmed by x-ray diffraction (XRD) analysis. The dependence of EL intensity for

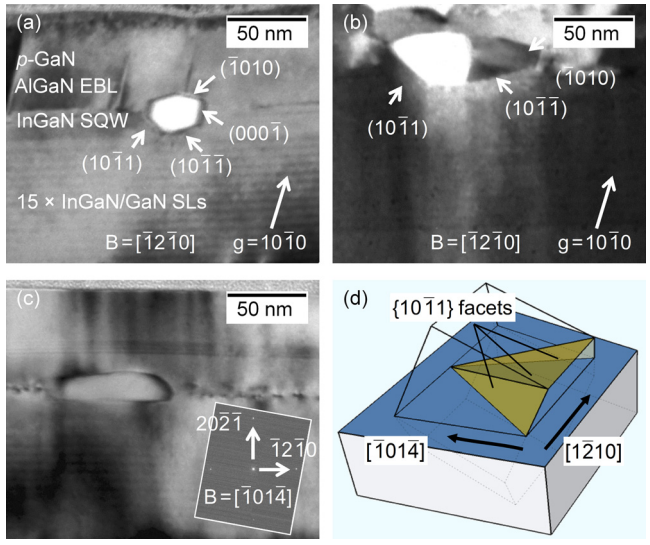

FIG. 2. (a) and (b) Two beam scattering contrast images for the 6 nm SQW (20$\bar{2}$1) LED in [1$\bar{2}$10] cross-sectional TEM with a diffraction condition of $\mathbf{g} = 10\bar{1}0$. (c) Multiple beam [$\bar{1}$014] cross-sectional TEM for the same sample. (d) Schematic view of one example of the defect on semipolar (20$\bar{2}$1) plane in a wurtzite crystal structure.

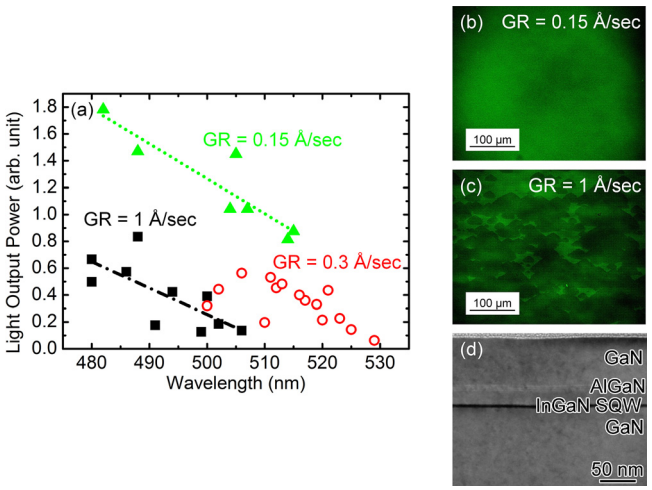

FIG. 3. (a) EL intensity as a function of wavelength for green semipolar $(20\bar{2}\bar{1})$ SQW InGaN LEDs grown at 1 Å/s, 0.3 Å/s, and 0.15 Å/s, respectively. FL microscopy images for $(20\bar{2}\bar{1})$ LEDs grown at (b) 0.15 Å/s and (c) 1 Å/s at 510 nm. (d) Multiple beam cross-sectional TEM taken around $[1\bar{2}10]$ zone axis for $(20\bar{2}\bar{1})$ LED grown at 0.15 Å/s at 510 nm.

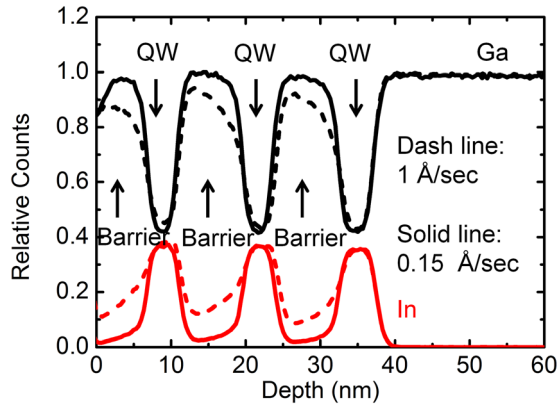

FIG. 5. SIMS measurements for the InGaN/GaN $(20\bar{2}\bar{1})$ QWs grown at 0.15 Å/s (solid line) and 1 Å/s (dashed line).

the devices on wavelength is summarized in Fig. 3(a). The EL intensities for all the devices decreased with increasing emission wavelength. The LEDs grown under slow growth rate demonstrated higher EL intensity and longer emission wavelength compared to those with faster growth rate, indicating higher quality QWs. Figures 3(b) and 3(c) demonstrate the FL images for LEDs with growth rate of 0.15 Å/s (b) and 1 Å/s (c) at an EL wavelength of 510 nm, respectively. Samples grown under slower growth rate (GR = 0.15 Å/s) showed a clear image in FL, indicating greatly reduced defect formation in the QW. This was also confirmed by TEM characterization on the slow growth rate sample [Fig. 3(c)]. In contrast, black triangular areas and void defects were found on samples grown at the fast growth rate (GR = 1 Å/s).

To further study the impact of growth rate on the epitaxial layer quality, QWs samples with 3 sets of undoped InGaN (3 nm)/GaN (10 nm) QW/barrier were grown on SP $(20\bar{2}\bar{1})$ GaN substrates with a growth rate of 0.15 Å/s and 1 Å/s, respectively. To ensure the accuracy for the material characterization, both the samples were grown with reduced indium composition. The PL wavelengths for the two samples were 488 nm and 492 nm, respectively, indicating a similar indium composition for both QWs. Black triangular defects were not observed for either the samples under FL measurement. Figures 4(a) and 4(b) demonstrate the AFM images of the two samples. Sample with slow active region growth rate (GR = 0.15 Å/s) showed a much smoother surface than that of the sample at fast growth rate (GR = 1 Å/s). This is possibly because the adatoms were unable to reach preferential incorporation cites at fast growth rate. The adatom diffusion length can be enhanced by reducing the growth rate, which may explain the improved the surface morphology for slow growth rate sample. In addition, the striated morphology was observed for both samples, indicating an in-plane diffusion anisotropy on the $(20\bar{2}\bar{1})$ plane. Such in-plane growth anisotropy has been reported on *m*-plane and $(20\bar{2}1)$ plane.[17–19] However, more systematic study is required to fully clarify this phenomenon.

Figure 5 demonstrates SIMS results for above two samples. Again black triangular defects were not observed for either the samples so that the effect of the defects on the accuracy of SIMS is minimal. In the InGaN QWs, two samples showed almost identical indium composition profile and is consistent with similar PL emission wavelength from both samples. For the GaN barrier, however, the sample with low growth rate showed a sharper barrier profile. A significant amount of indium was present in the nominal GaN barriers for the sample with fast growth rate, resulting in a barriers profile with higher indium composition. These results may be related to the indium condensation and droplets formation during the growth. Jiang *et al.* studied indium condensation boundaries for MOCVD InGaN growth and showed that growth parameters such as TMI pressure and substrate temperature have a significant effect on both condensation and

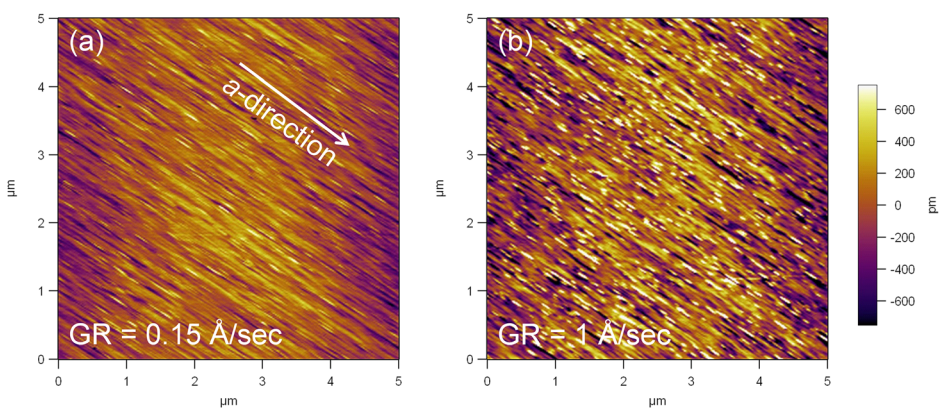

FIG. 4. AFM images of the InGaN/GaN $(20\bar{2}\bar{1})$ QWs grown at (a) 0.15 Å/s and (b) 1 Å/s.

adsorption of indium.[20] It is possible that at the fast growth conditions, the indium condensation becomes energetically favorable, which contributes to the poor structure uniformity and structure degradation in the active region. Slow growth, on the other hand, leads to more ideal QW and barrier profile with stable compositions. In addition, it was recently discovered that the after-active-region *p*-GaN growth also affects the formation of black triangular and void defects for SP $(20\bar{2}1)$ laser structures.[21] Due to the complexity of these defects, many of their physical properties are still largely unknown. More material studies are therefore required to fully understand this problem.

In conclusion, void defects with $\{10\bar{1}1\}$, $\{10\bar{1}0\}$, and $\{000\bar{1}\}$ facets were identified for SP $(20\bar{2}\bar{1})$ InGaN/GaN QWs emitting in the green spectral region. These defects can be effectively suppressed using a slow growth rate for the active region, resulting in devices with higher power and longer emission wavelength. QWs of slow growth rate also showed improved surface morphology and compositional profile.

The authors acknowledge the support of Solid State Lighting and Energy Center at UCSB. A portion of this work was done in the UCSB nanofabrication facility, part of the NSF funded NNIN. This work made use of MRL Central Facilities supported by the MRSEC Program of the National Science Foundation under Award No. DMR 1121053.

[1]S. Nakamura, MRS Bull. **34**, 101 (2009).
[2]J. W. Raring, M. C. Schmidt, C. Poblenz, Y. C. Chang, M. J. Mondry, B. Li, J. Iveland, B. Walters, M. R. Krames, R. Craig, P. Rudy, J. S. Speck, S. P. DenBaars, and S. Nakamura, Appl. Phys. Express **3**, 112101 (2010).
[3]Y. Enya, Y. Yoshizumi, T. Kyono, K. Akita, M. Ueno, M. Adachi, T. Sumitomo, S. Tokuyama, T. Ikegami, K. Katayama, and T. Nakamura, Appl. Phys. Express **2**, 082101 (2009).
[4]Y. D. Lin, S. Yamamoto, C. Y. Huang, C. L. Hsiung, F. Wu, K. Fujito, H. Ohta, J. S. Speck, S. P. Denbaars, and S. Nakamura, Appl. Phys. Express **3**, 082001 (2010).
[5]P. Waltereit, O. Brandt, A. Trampert, H. T. Grahn, J. Menniger, M. Ramsteiner, M. Reiche, and K. H. Ploog, Nature (London) **406**, 865 (2000).
[6]F. Bernardini and V. Fiorentini, Phys. Status Solidi B **216**, 391 (1999).
[7]Y. Zhao, J. Sonoda, I. Koslow, C. C. Pan, H. Ohta, J. S. Ha, S. P. DenBaars, and S. Nakamura, Jpn. J. Appl. Phys. **49**, 070206 (2010).
[8]F. Wu, Y. D. Lin, A. Chakraborty, H. Ohta, S. P. DenBaars, S. Nakamura, and J. S. Speck, Appl. Phys. Lett. **96**, 231912 (2010).
[9]S. Yamamoto, Y. Zhao, C. C. Pan, R. B. Chung, K. Fujito, J. Sonoda, S. P. Denbaars, and S. Nakamura, Appl. Phys. Express **3**, 122102 (2010).
[10]Y. Zhao, T. Tanaka, Q. Yen, C. Y. Huang, R. B. Chung, C. C. Pan, K. Fujito, D. Feezell, C. G. Van de Walle, J. S. Speck, S. P. DenBaars, and S. Nakamura, Appl. Phys. Lett. **99**, 051109 (2011).
[11]Y. Zhao, S. Tanaka, C. C. Pan, K. Fujito, D. Feezell, J. S. Speck, S. P. DenBaars, and S. Nakamura, Appl. Phys. Express **4**, 082104 (2011).
[12]Y. Zhao, Q. Yan, C. Y. Huang, S. C. Huang, P. S. Hsu, S. Tanaka, C. C. Pan, Y. Kawaguchi, K. Fujito, C. G. Van de Walle, J. S. Speck, S. P. DenBaars, S. Nakamura, and D. Feezell, Appl. Phys. Lett. **100**, 201108 (2012).
[13]C. Y. Huang, M. T. Hardy, K. Fujito, D. Feezell, J. S. Speck, S. P. DenBaars, and S. Nakamura, Appl. Phys. Lett. **99**, 241115 (2011).
[14]X. H. Wu, C. R. Elsass, A. Abare, M. Mack, S. Keller, P. M. Petroff, S. P. DenBaars, J. S. Speck, and S. J. Rosner, Appl. Phys. Lett. **72**, 692 (1998).
[15]A. B. Yankovichi, A. V. Kvit, X. Li, F. Zhang, V. Avrutin, H. Y. Liu, N. Izyumskaya, U. Ozgur, H. Morkovc, and P. M. Voyles, J. Appl. Phys. **111**, 023517 (2012).
[16]Y. Kawaguchi, C. Y. Huang, Y. R. Wu, Y. Zhao, S. P. DenBaars, and S. Nakamura, "Semipolar $(20\bar{2}1)$ Single-Quantum-Well Red Light-Emitting Diodes with a Low Forward Voltage", (unpublished).
[17]C. Q. Chen, M. E. Gaevski, W. H. Sun, E. Kuokstis, J. P. Zhang, R. S. Q. Fareed, H. M. Wang, J. W. Yang, G. Simin, and M. A. Khan, Appl. Phys. Lett. **81**, 3194 (2002).
[18]L. Lymperakis and J. Neugebauer, Phys. Rev. B **79**, 241308 (2009).
[19]S. Ploch, T. Wernicke, J. Thalmair, M. Lohr, M. Pristovsek, J. Zweck, M. Weyers, and M. Kneissl, J. Cryst. Growth **356**, 70 (2012).
[20]F. Jiang, R. V. Wang, A. Munkholm, S. K. Streiffer, G. B. Stephenson, P. H. Fuoss, K. Latifi, and C. Thompson, Appl. Phys. Lett. **89**, 161915 (2006).
[21]M. T. Hardy, F. Wu, C. Y. Huang, Y. Zhao, D. Feezell, J. S. Speck, S. Nakamura, and S. P. DenBaars, "Impact of p-GaN Temperature and AlGaN Barrier Composition on $(20\bar{2}1)$ Green Laser Diodes", (unpublished).